ATTENTION FOR FINE-GRAINED CATEGORIZATION

Pierre Sermanet, Andrea Frome, Esteban Real
Google, Inc.
{sermanet,afrome,ereal,}@google.com

ABSTRACT

This paper presents experiments extending the work of Ba et al. (2014) on recurrent neural models for attention into less constrained visual environments, specifically fine-grained categorization on the Stanford Dogs data set. In this work we use an RNN of the same structure but substitute a more powerful visual network and perform large-scale pre-training of the visual network outside of the attention RNN. Most work in attention models to date focuses on tasks with toy or more constrained visual environments, whereas we present results for fine-grained categorization better than the state-of-the-art GoogLeNet classification model. We show that our model learns to direct high resolution attention to the most discriminative regions without any spatial supervision such as bounding boxes, and it is able to discriminate fine-grained dog breeds moderately well even when given only an initial low-resolution context image and narrow, inexpensive glimpses at faces and fur patterns. This and similar attention models have the major advantage of being trained end-to-end, as opposed to other current detection and recognition pipelines with hand-engineered components where information is lost. While our model is state-of-the-art, further work is needed to fully leverage the sequential input.

1 INTRODUCTION

This work presents experiments extending the work of Ba et al. (2014) on recurrent neural models for attention into less constrained visual environments, specifically fine-grained categorization on the Stanford Dogs data set. Ba et al. (2014) tackles the challenging problem of sequence prediction in simplified visual settings (MNIST and Street View House Numbers) using a recurrent model of attention similar to Mnih et al. (2014). Complementary to that work, we are addressing the simpler task of classification but in a visual environment with significant clutter and occlusion, variations in lighting and pose, and a more difficult class discrimination task. Previous work in learned visual attention models has tackled a number of computer vision problems and demonstrated the benefits of various attention mechanisms, though most of the work has been focused on toy or more constrained environments, such as detecting simple shapes (Schmidhuber & Huber, 1991), tasks based on MNIST digits (Larochelle & Hinton, 2010; Bazzani et al., 2011; Denil et al., 2012; Ranzato, 2014; Mnih et al., 2014), the vision-control game of "catch" (Mnih et al., 2014), expression classification for 100×100 aligned faces (Larochelle & Hinton, 2010; Zheng et al., 2014), detection of frontal faces (Tang et al., 2013), tracking of hockey players (Bazzani et al., 2011; Denil et al., 2012) and gesture recognition (Darrell & Pentland, 1996). Most recently, two papers have explored attention mechanisms for more complex visual input: Gonzalez-Garcia et al. (2014) presented an attention-like model for detection of chairs, people, cars, doors, and tables from SUN2012 images (Xiao et al., 2010); Xu et al. (2015) applied two different neural network visual attention models to the task of caption generation for MSCOCO images (Lin et al., 2014).

Recent work in object detection (Szegedy et al., 2014b; Girshick et al., 2014) and fine-grained categorization (Zhang et al., 2014) use candidate object or part proposals as a precursor to a more expensive classification stage. In these systems, the proposals are generated from a bottom-up segmentation as in Girshick et al. (2014) or from a separate neural network as in Szegedy et al. (2014b). As in our work, these pipelines are able to process candidate regions for classification at a higher resolution and save processing by focusing on a restricted set of regions. Drawbacks to these systems are that they consist of independent processing steps with engineered connections between them

where information is lost. As an example, they either do not aggregate evidence from independent candidate image regions or do so with an ad hoc technique. They also lose rich information between the candidate proposal and classification parts of the pipeline. In contrast, our models and others with similar structure are trained end-to-end to incorporate information across observations, which can be expected to yield a better final result.

Figure 1: Three classes from the Dogs data set that are difficult to tell apart due to high intra-class variability and high similarity across classes. The lines show the class boundaries; the classes are Eskimo Dog on the left, Malamute in the center, and Siberian Husky on the right. Of the 120 classes in Stanford Dogs, our model performs worst on Siberian Husky.

We apply the visual attention model from Ba et al. (2014) to the Stanford Dogs fine-grained categorization task (Khosla et al., 2011), choosing to perform the task without using the provided bounding boxes for training or testing. This amounts to learning to simultaneously localize and classify objects within scenes despite difficult class boundaries, large variations in pose and lighting, varying and cluttered backgrounds, and occlusion (Figure 1). Fine-grained categorization is a natural proving ground for attention-based models. When performing classification at the sub-category level, e.g. German Shepherd versus Poodle, the background is often uncorrelated with class and acts as a distraction to the primary task. As a result, several hand-crafted vision pipelines use provided bounding boxes to isolate the object of interest or may perform segmentation of the object from the background, e.g. Parkhi et al. (2011); Chai et al. (2013); Angelova & Zhu (2013). Attention models could address this challenge by learning to focus processing and discriminatory power on the parts of the image that are relevant for the task without requiring expensive hand-labeled bounding boxes. In addition to ignoring the distractors in the image, a good attention model could learn to focus processing power on the specific features of the objects that help to tell them apart, for example the face, ears, and particular fur patterns for dogs. Future versions of this model could potentially also choose the scale at which to examine details.

2 MODEL DESCRIPTION

The structure of our model is nearly the same as that presented in Ba et al. (2014) with a few differences; we give an overview of their model here and describe the ways in which our model differs. We refer the reader to that work for a more in-depth description of the network choices and training procedure.

Figure 2 shows the structure of the model. The system as a whole takes as input an image of any size and outputs N-way classification scores using a softmax classifier, which is a similar task to the finding digits and digit addition tasks in Ba et al. (2014). The model is a recurrent neural network, with N steps that correlate with N "glimpses" into the input image. At step n, the model receives row and column coordinates l_{n-1}, which describe a point in the input image. The network extracts a multi-resolution patch from the input image at those coordinates, passes the pixels through fully-
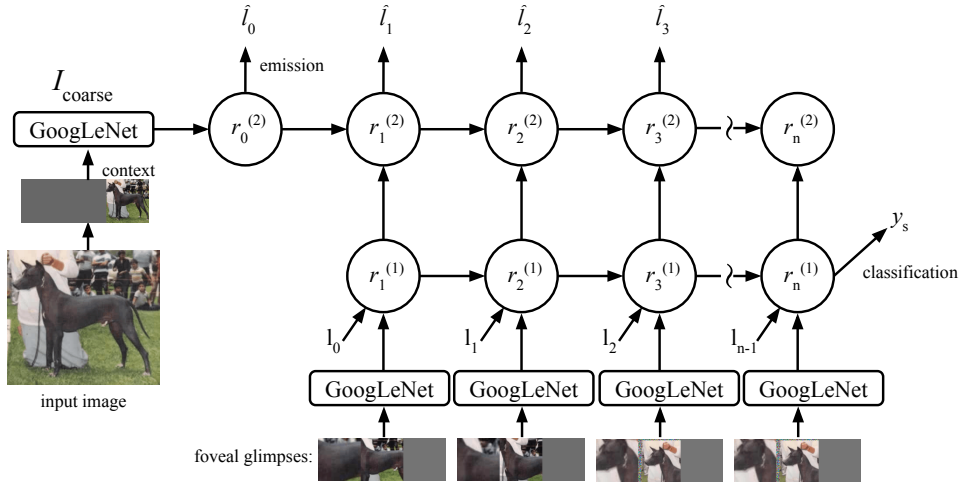
2

Figure 2: Diagram of the model. The grayed-out boxes denote resolutions not in use; in our experiments the context is always a low-resolution patch, while each glimpse can be any combination of the low-, medium-, and high-resolution patches.

connected layers which combine with activations from the previous glimpse step, and either outputs coordinates $\hat{l}_n$ for the next glimpse or a final classification y_s.

The structure of the glimpse images is shown in Figure 3. Each glimpse is a multi-resolution image created by extracting patches at varying sizes, resizing them all to 96×96, and concatenating them side-by-side. The goal is to emulate a "foveal" structure with the sharpest part of the image in the center and lower resolution toward the periphery. The top row shows glimpses for a 2-resolution model and the bottom row for a 3-resolution model. The high-resolution patch is extracted from a square that is a fixed size for a given image (more on scale selection below). The medium-resolution patch is from a square that is twice the length on a side of the high-resolution patch, and the low-resolution patch is twice the length of the medium-resolution patch on a side. For example, if the high resolution patch is 100×100, then the medium- and low-resolution patches are 200×200 and 400×400, respectively. Where an extraction box extends off the edge of the image, we fill the pixels with random noise. Figure 3 shows composite images which are a helpful visualization to understand what pixels the network sees in aggregate, though the network is not presented with them in this form; these images are generated from the glimpse pixels by displaying at each pixel the highest-resolution pixel available in any glimpse, and any pixels not captured by the glimpses are filled with noise.

The model begins processing from a "context image", which is a square low-resolution patch from the input image that is the same size as our low-resolution glimpse patch and is also resized to 96×96. The location of the context image is chosen randomly in training, but it is centered during inference when it captures the central square of the image. The context image is used by layer $r_o^{(2)}$ to produce the first glimpse location l_0 and can influence the selection of subsequent glimpse locations through the recurrent connections between the $r_n^{(2)}$ layers along the "top deck" of the model. However, the double-decker structure prevents the context image from having a pathway to the classifier except through the l_n coordinates. See Ba et al. (2014) for more discussion about this design choice. In training, the $r_n^{(2)}$ layers that produce the $\hat{l}_n$ coordinates are trained with a mix of backpropagation from the connection to layer $r_{n+1}^{(1)}$ and a policy gradient update.

There are four major differences between our system and the classification-type models from Ba et al. (2014). First, there is wide variation in image size across our data set, however the size of the objects scales with the image size most of the time. To be robust to input image size, our multi-resolution patches are sized relative to the input image. In our experiments, a side of the high-
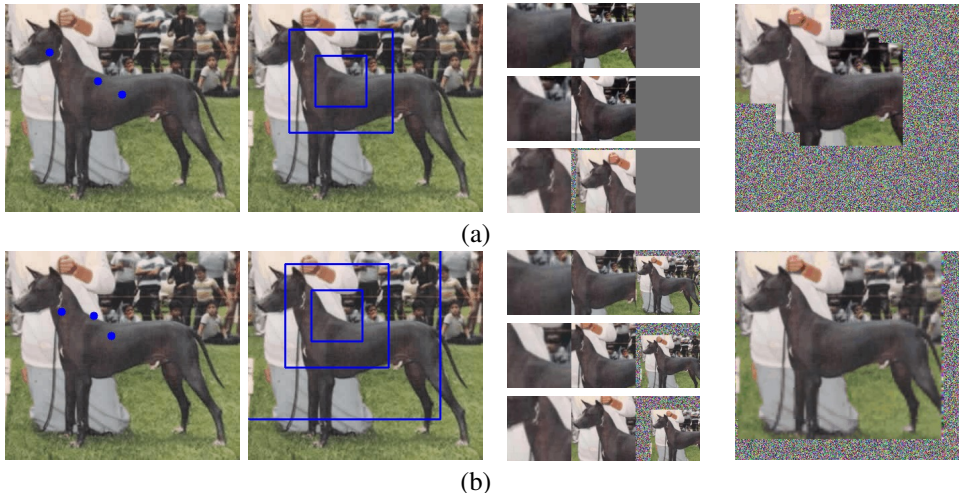
3

(a)

(b)

Figure 3: Visualizations of 2-resolution (a) and 3-resolution (b) glimpses on an image from our validation set, with learned fixation points. For each the glimpse images are in order, from top to bottom, and the box diagram corresponds to the second glimpse. The composite image is created from all three glimpses. The context image is not shown but is always the same resolution and size as the low-resolution glimpse patches shown in (b).

resolution square patch is $1/4$ the shorter dimension of the input image, making the sides of the medium- and low-resolution patches $1/2$ and the full length of the image's short side, respectively.

Second, we use a "vanilla" RNN instead of an LSTM, where $r_n^{(1)}$ and $r_n^{(2)}$ at glimpse n each consist of 4,096 nodes, and $r_n(i)$ is fully-connected to $r_{n+1}(i)$ for $i = 1, 2$. Third, instead of element-wise multiplying the outputs of the glimpse visual core $G_{image}(x_n|W_{image})$ and $G_{loc}(l_n|W_{loc})$, our model linearly combines them by concatenating their outputs and passing through a fully-connected layer. Future experiments will incorporate both of these variations.

The final and largest difference is that we replace the visual glimpse network $G_{image}(x_n|W_{image})$ described in Ba et al. (2014) with a more powerful visual core based on the "GoogLeNet" model (Szegedy et al., 2014a) that won the ILSVRC 2014 classification challenge. We start from a GoogLeNet model that we pre-trained on the ImageNet 1000-way task on a subset of the ILSVRC 2012 training data (Russakovsky et al., 2014) (more on our use of this data set below).

We then fine-tune the visual network outside of the RNN model on ILSVRC images using random multi-scale patches as input and targeting the ImageNet 1000-way classification labels. In this stage of training, we replicate the visual model for each input scale, yielding 3 "towers" which share parameters and join their outputs in different combinations with depth-concatenating layers (Figure 4). All towers are jointly trained by back-propagating the loss from multiple 1000-way softmax classifiers (called "heads") as shown in the figure. This multi-headed training model ensures each tower remains independently relevant even if another tower is more informative. We have found that if taken independently, the lowest-resolution patch typically yields best results and learning might rely on it solely otherwise.

We initially used a truncated version of GoogLeNet as the visual core of the RNN because the full model is designed for 224×224 inputs and if applied to 96×96 inputs, the subsampling and pooling layers cause the final output to be too small for our purposes. To remedy this, we initially chopped off the last two "inception" layers, skipping five convolutional layers and an average-pooling layer. We later discovered a large gain in performance by changing the stride of the first convolution of the network from two to one and restoring the visual network to its full depth. Stride-1 convolutions were historically used in early deep learning works, however Krizhevsky et al. (2012) later popularized strides of two in early layers for efficiency reasons. In our experiments, we changed the stride only in the fine-tuning phase, starting from a pre-trained model with a stride of two. Although it is not obvious that changing the stride of a pre-trained model should work, when incorporated with the
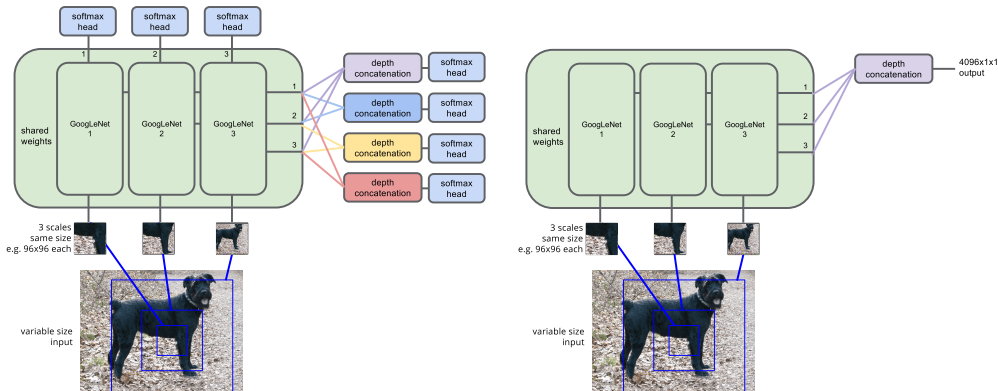
4

Figure 4: Pre-training of the visual core (left) and inference within the RNN (right).

RNN, the best performance of the three-resolution, three-glimpse attention model increased from 68% to 76.8%.

During training of the attention model, we remove all training heads and take the output of the depth concatenation of multiple towers as glimpse input as shown in Figure 4. For this work, we hold the visual core's parameters fixed during attention model training. We pre-train with all three resolutions, but when used in the RNN, we vary across experiments which subsets of the resolutions are used, so the training regime in those experiments is slightly different than testing.

In all stages of training for the attention RNN and our experimental baselines, we use a subset of the ILSVRC 2012 training set from which we removed the Stanford Dogs test images as well as the Dogs images that we use for validation. We refer to this in our experimental section as the "de-duped" ILSVRC data set. Pre-training with de-duped data instead of the original set does make a small difference in performance: we saw a drop of 3% accuracy in the full GoogLeNet baseline model when trained with de-duped data relative to one trained with the full ILSVRC 2012 training set.

Finally, it is worth noting that when fine-tuning the visual core, we did not use the Stanford Dogs training set, and since the parameters of the visual core are held fixed while training the RNN on Dogs, this means the powerful visual processing component in the RNN is not trained on the final task. We performed an experiment with a visual core fine-tuned on the Stanford Dogs training data, and we did not see an increase in performance, demonstrating again that the final RNN model is fairly robust to the pre-training and fine-tuning procedure.

3 EXPERIMENTAL RESULTS

We trained and evaluated our model on the Stanford Dogs fine-grained categorization data set (Khosla et al., 2011). The task is to categorize each of 8,580 test images as containing one of 120 dog breeds. The training set consists of 100 images per class, and the test images are unevenly distributed across classes, averaging about 71 test images per class. The training and test sets both include bounding boxes that provide a tight crop around the target dog, and while the best results we know of in the literature use the bounding boxes both in training and testing, we use neither the training nor testing boxes. We follow the practice common in the literature of augmenting the training set by reflecting the images along the vertical axis. Our model starts from the full images, without cropping, reshaping, or scaling. We performed experiments and chose hyperparameters using an 80/20 training/validation split of the Stanford Dogs training set. We selected hyperparameters (e.g. learning rate, sample variance) using the 20% validation set then trained on the full training set, and we only performed final evaluation on the Dogs test set on our selected hyperparameters.

The background in the images is not highly correlated with the class label, so any method not using the bounding boxes needs to localize the object of interest in order to classify it. This is a nice task to explore for our attention model in a couple ways: (1) the model can use the context image in order to focus its glimpses on the object of interest, and (2) we can intuit which parts of the image the model

Table 1: Results on Stanford Dogs for (a) our RNN model and (b) our GoogLeNet baselines and previous state-of-the-art results, measured by mean accuracy percentage (mA) as described in Chai et al. (2013). The GoogLeNet baseline models were pre-trained on the de-duped ILSVRC 2012 training set and fine-tuned with the Stanford Dogs training set. Results marked with a star indicate use of tight ground truth bounding boxes around the dogs in training and testing.

# glimpses	1	2	3		
high res only	43.5	48.3	49.6	Yang et al. (2012)*	38.0
medium res only	70.1	72.3	72.8	Chai et al. (2013)*	45.6
low res only	70.3	70.1	70.7	Gavves et al. (2013)*	50.1
high+medium res	70.7	72.6	72.7	GoogLeNet 96×96	58.8
3-resolution	76.3	76.5	**76.8**	GoogLeNet 224×224	**75.5**
	(a)			(b)	

should observe to make a prediction. With many other natural image object classification data sets, such as ImageNet, the signal from the surrounding context is mixed with the object for classification (e.g. boats are expected to be surrounded by water). The size of the data set is also more suitable to a deep learning method than most other available fine-grained data sets, though Caltech-UCSD Birds 2011 (Wah et al., 2011) is similar in size with 12,000 training images for 200 categories.[1] Lastly, it remains a difficult data set, with a large amount of intra-class variation, similarity across classes, and large variation in pose, lighting, and background (Figure 1).

Table 1(a) shows the mean accuracy (mA) for different combinations of resolutions and number of glimpses. We experimented with high, medium, and low resolutions individually, medium and high combined, and all three resolutions and with one, two, and three glimpses. The table also shows previously published results on the data set[2]. Versions of our model that use medium and low resolution patches outperform state-of-the-art results. When using only two small high-resolution patches from the image, our model matches the best published result. All previously published results shown use ground truth bounding boxes for training and testing while our model does not.

While the high-resolution single-glimpse model has the lowest performance of the set, visualizations of the selected glimpse locations show that it is learning to take a good first action (Figure 5). These are fairly representative of the behavior of the model, which most frequently chooses a patch on or near the dog's face. While it may make an informative first glimpse, it is often not able to correctly classify the dog from that single sample. It is important to note that the model automatically learned to focus on the most discriminative features such as faces and fur without ever receiving spatial clues such as bounding boxes. This is pretty remarkable in that bounding boxes are usually required for good performance on this task, and obtaining bounding boxes at scale is difficult and expensive. It also raises the possibility of attention models providing a signal for detection without labeled bounding boxes. The figure shows two images where it classified the dog correctly in green, and one in red where it assigned an incorrect label. One pathological pattern we noticed is that if there are two dogs in the image, it often chooses a patch that is halfway between the two, which is likely due to the regression-style output of the glimpse coordinates which may encourage the model to output the average of two predicted targets. A set of randomly chosen examples is shown in the appendix with Figure 6.

Comparisons to results not using deep learning do not give a good sense of the strength of the model, however. In the last couple years deep nets have been winning the ILSVRC classification challenge by a significant margin, so it may be expected that a deep neural net would outperform the existing results. To address this we also evaluated GoogLeNet on the full image without the attention

---

[1]We have not yet experimented with Caltech-UCSD Birds 2011, but the approach here should apply nicely.

[2]Missing from the results are entries to the FGComp 2013 fine-grained competition. There are high-performing entries from deep learning models in the dogs category, though to our knowledge these models have not been published. *CognitiveVision* and *CafeNet* scored 61% and 57% on the challenge, respectively, using bounding boxes both in training and testing. The challenge training set is from Stanford Dogs, but the test set is independent, the class labels have not been made public, and the evaluation server is no longer running. As such, we cannot compare directly to these numbers, but we have been told anecdotally that scores on the FGComp 2013 challenge tend to be about 10% absolute lower than on the Stanford Dogs test set.
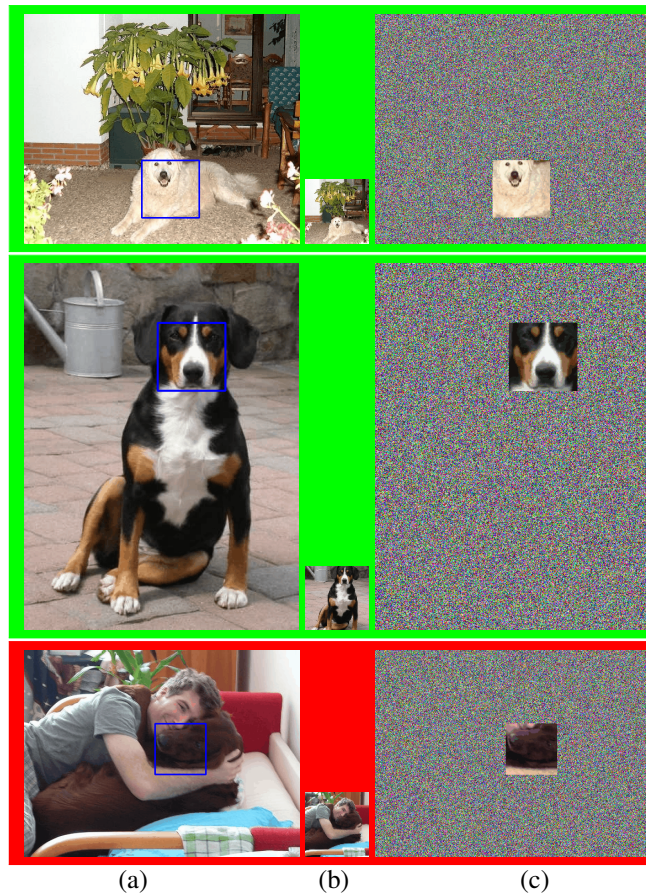
Figure 5: Selected examples of the high-resolution, one-glimpse model run on the validation set. The system takes (a) the original image, subsamples it to create (b) the context image, and uses the context to select (c) a single high resolution glimpse. The outline of the high-resolution glimpse is also shown on the full image in (a) for context. Rows surrounded by green were correctly classified, while red indicates a classification error. Note that while the bottom example is misclassified, the model still learned to look at the dog face despite clutter, occlusion, and an uncommon pose. See Figure 6 for a random selection of results.

RNN. We experimented with two baseline versions of GoogLeNet: "full" and "low-resolution". The full GoogLeNet uses the same architecture as in Szegedy et al. (2014a) and is trained and tested on 224×224 padded versions of the full Dog images. This is the strongest of the two baselines. The low-resolution GoogLeNet has the same architecture as our RNN visual core and also takes 96×96 inputs and uses a stride of one for the first convolution. It does not have three input scales like the RNN visual core but instead takes the full image with padding that centers it. The low-resolution GoogLeNet input is close in resolution to the low-resolution foveal input to our attention model. Both versions were pre-trained using the de-duped ILSVRC 2012 data set, then the top fully-connected layer and softmax layers were resized and reinitialized, and the full model was trained to convergence on the Dogs training set. In addition to the mirroring applied for RNN training, brightness and color transformations were also applied to the training images for the baselines. Unlike Szegedy et al. (2014a), for this comparison we did not average across patches or different GoogLeNet models.

Our three-resolution, one-glimpse attention model reached 76.3% mA compared to 75.5% for the full GoogLeNet model (1(b)). This version of the attention model gets three 96×96 inputs it can use for classification and the 96×96 context image for choosing the position of the one glimpse. Compared to the 224×224 input to GoogLeNet, we perform better with 73% of the pixels. This doesn't reduce the amount of computation, however, because the attention model uses a stride of one in the first convolutional layer compared to two in the full GoogLeNet. With three glimpses, the performance increases slightly to 76.8%, though this almost triples the number of pixels input[3]. With only medium and high resolution inputs (72.7%, three glimpses), the attention model is nearing the performance of full GoogLeNet with 55% of the pixels.

A comparison between the low-resolution GoogLeNet (58.8%) and our low resolution attention model (70.3%, one glimpse) shows that the increase in convolution stride does not account for the strong performance because both models share the same visual network and similar resolution inputs (depending on ratio of the long and short sides of the image). This indicates the large difference in performance is due to the network choosing an informative part of the image to use as input for classification.

Lastly, it is interesting to compare one-, two-, and three- glimpse results for different resolution inputs. Using three resolutions, the performance only increases slightly from 76.3% for one glimpse to 76.8% for three. One likely cause is that the three-resolution glimpse contains enough information from the full image that the information gained from additional glimpses is minimal. An additional piece of evidence is that the performance order of low- and medium-only resolution models swap when going from one to two glimpses. We ran the high resolution-only glimpse experiment to test this; the results for one, two, and three glimpses are 43.5%, 48.3%, and 49.6%, respectively, demonstrating that when the amount of information in each glimpse is restricted, the model benefits more from several glimpses. However, the improvement with increased number of glimpses flattens quickly, indicating that the model has limited capacity to make use of more than two or three glimpses. One hypothesis is the RNN is not passing enough of the information from the early glimpses along to the classification layer. It is future work to explore using LSTM cells and increasing the recurrent capacity of the network.

REFERENCES

Angelova, Anelia and Zhu, Shenghuo. Efficient object detection and segmentation for fine-grained recognition. In *CVPR'13: IEEE Conference on Computer Vision and Pattern Recognition*, June 23-28, 2013. doi: 10.1109/CVPR.2013.110.

Ba, Jimmy, Mnih, Volodymyr, and Kavukcuoglu, Koray. Multiple Object Recognition with Visual Attention. *CoRR*, TBD, 2014. URL http://arxiv.org/abs/1412.7755.

Bazzani, Loris, de Freitas, Nando, Larochelle, Hugo, Murino, Vittorio, and Ting, Jo-Anne. Learning attentional policies for object tracking and recognition in video with deep networks. In *ICML'11: Proceedings of the 28th International Conference on Machine Learning*, pp. 937–944. ACM, 2011.

---

[3]For a fairer comparison between multiple-glimpse attention and GoogLeNet, we would ideally take an equal number of random crops as input to GoogLeNet and average the outputs.

Chai, Yuning, Lempitsky, Victor, and Zisserman, Andrew. Symbiotic Segmentation and Part Localization for Fine-Grained Categorization. In *ICCV'13: IEEE International Conference on Computer Vision*, 2013.

Darrell, T. and Pentland, A. Active gesture recognition using learned visual attention. In *Advances in Neural Information Processing Systems 8*. MIT Press, Cambridge MA, 1996.

Denil, Misha, Bazzani, Loris, Larochelle, Hugo, and de Freitas, Nando. Learning where to attend with deep architectures for image tracking. *Neural Comput.*, 24(8):2151–2184, 2012. ISSN 0899-7667.

Gavves, Efstratios, Fernando, Basura, Snoek, Cees, Smeulders, Arnold, and Tuytelaars, Tinne. Fine-Grained Categorization by Alignments. In *ICCV'13: IEEE International Conference on Computer Vision*, 2013.

Girshick, Ross, Donahue, Jeff, Darrell, Trevor, and Malik, Jitendra. Rich feature hierarchies for accurate object detection and semantic segmentation. In *Proceedings of the IEEE Conference on Computer Vision and Pattern Recognition (CVPR)*, 2014.

Gonzalez-Garcia, Abel, Vezhnevets, Alexander, and Ferrari, Vittorio. An active search strategy for efficient object detection. *CoRR*, abs/1412.3709, 2014. URL http://arxiv.org/abs/1412.3709.

Khosla, Aditya, Jayadevaprakash, Nityananda, Yao, Bangpeng, and Fei-Fei, Li. Novel Dataset for Fine-Grained Image Categorization. In *First Workshop on Fine-Grained Visual Categorization, CVPR'11: IEEE Conference on Computer Vision and Pattern Recognition*, June 2011.

Krizhevsky, Alex, Sutskever, Ilya, and Hinton, Geoffrey E. Imagenet classification with deep convolutional neural networks. In *Advances in neural information processing systems*, pp. 1097–1105, 2012.

Larochelle, Hugo and Hinton, Geoffrey E. Learning to combine foveal glimpses with a third-order boltzmann machine. In *NIPS'10: Advances in Neural Information Processing Systems 23*, pp. 1243–1251. Curran Associates, Inc., 2010.

Lin, Tsung-Yi, Maire, Michael, Belongie, Serge, Hays, James, Perona, Pietro, Ramanan, Deva, Dollár, Piotr, and Zitnick, C. Lawrence. Microsoft COCO: common objects in context. *CoRR*, abs/1405.0312, 2014. URL http://arxiv.org/abs/1405.0312.

Mnih, Volodymyr, Heess, Nicolas, Graves, Alex, and kavukcuoglu, koray. Recurrent models of visual attention. In *Advances in Neural Information Processing Systems 27*, pp. 2204–2212. Curran Associates, Inc., 2014.

Parkhi, Omkar M., Vedaldi, Andrea, Jawahar, C. V., and Zisserman, Andrew. The Truth About Cats and Dogs. In *ICCV'11: IEEE International Conference on Computer Vision*, 2011.

Ranzato, Marc'Aurelio. On Learning Where To Look. *CoRR*, abs/1405.5488, 2014. URL http://arxiv.org/abs/1405.5488.

Russakovsky, Olga, Deng, Jia, Su, Hao, Krause, Jonathan, Satheesh, Sanjeev, Ma, Sean, Huang, Zhiheng, Karpathy, Andrej, Khosla, Aditya, Bernstein, Michael, Berg, Alexander C., and Fei-Fei, Li. ImageNet Large Scale Visual Recognition Challenge, 2014.

Schmidhuber, Jrgen and Huber, Rudolf. Learning to generate artificial fovea trajectories for target detection. *International Journal of Neural Systems*, pp. 135–141, 1991.

Szegedy, Christian, Liu, Wei, Jia, Yangqing, Sermanet, Pierre, Reed, Scott, Anguelov, Dragomir, Erhan, Dumitru, Vanhoucke, Vincent, and Rabinovich, Andrew. Going deeper with convolutions. *CoRR*, abs/1409.4842, 2014a. URL http://arxiv.org/abs/1409.4842.

Szegedy, Christian, Reed, Scott, Erhan, Dumitru, and Anguelov, Dragomir. Scalable, high-quality object detection. *CoRR*, abs/1412.1441, 2014b. URL http://arxiv.org/abs/1412.1441.

Tang, Yichuan, Srivastava, Nitish, and Salakhutdinov, Ruslan. Learning generative models with visual attention. *CoRR*, abs/1312.6110, 2013. URL `http://arxiv.org/abs/1312.6110`.

Wah, Catherine, Branson, Steve, Welinder, Peter, Perona, Pietro, and Belongie, Serge. The Caltech-UCSD Birds-200-2011 Dataset. Technical Report CNS-TR-2011-001, California Institute of Technology, 2011.

Xiao, Jianxiong, Hays, James, Ehinger, Krista A., Oliva, Aude, and Torralba, Antonio. SUN database: Large-scale scene recognition from abbey to zoo. In *Computer Vision and Pattern Recognition (CVPR)*, 2010. URL `http://dblp.uni-trier.de/db/conf/cvpr/cvpr2010.html#XiaoHEOT10`.

Xu, Kelvin, Ba, Jimmy, Kiros, Ryan, Cho, Kyunghyun, Courville, Aaron, Salakhutdinov, Ruslan, Zemel, Richard, and Bengio, Yoshua. Show, Attend and Tell: Neural Image Caption Generation with Visual Attention. *CoRR*, arXiv:1502.03044, 2015. URL `http://arxiv.org/abs/1502.03044`.

Yang, Shulin, Bo, Liefeng, Wang, Jue, and Shapiro, Linda G. Unsupervised Template Learning for Fine-Grained Object Recognition. In *NIPS'12: Advances in Neural Information Processing Systems*, December 2012.

Zhang, Ning, Donahue, Jeff, Girshick, Ross B., and Darrell, Trevor. Part-based R-CNNs for Fine-grained Category Detection. *CoRR*, abs/1407.3867, 2014. URL `http://arxiv.org/abs/1407.3867`.

Zheng, Yin, Zemel, Richard S., Zhang, Yu-Jin, and Larochelle, Hugo. A Neural Autoregressive Approach to Attention-based Recognition. *IJCV'14: International Journal of Computer Vision*, pp. 1–13, 2014.

A   RANDOM VALIDATION SAMPLES

Figure 6 shows ten randomly-selected validation examples from four different versions of the attention model: three-resolution (low, medium, high) with three glimpses, three-resolution with one glimpse, high-resolution only with three glimpses, and high-resolution with one glimpse. For each model and input, on the left it shows the original image with dots at the centers of the glimpses, and on the right it shows a composite image. Green borders indicate a correct classification, and red borders indicate an error. The leftmost column is the most accurate system, however it is interesting to see that while the rightmost column is least accurate, the model correctly directs its attention to the most informative areas (dog faces) but lacks enough information to classify correctly. It is also interesting to note in the last sample, the rightmost model correctly classifies a breed given a non-face feature, showing that the system has learned to identify a variety of useful parts instead of relying solely on facial features.

Figure 6: Ten randomly-selected validation samples from four different model variations. See text for details.